Paper No. 2072. (quote when citing this article)
Eleventh World Conference on Earthquake Engineering
ISBN: 0 08 042822 3

CONSISTENT INFINITESIMAL FINITE-ELEMENT CELL METHOD TO MODEL UNBOUNDED SOIL—A BOUNDARY FINITE-ELEMENT PROCEDURE

JOHN P. WOLF and CHONGMIN SONG

Institute of Hydraulics and Energy, Department of Civil Engineering, Swiss Federal Institute of Technology Lausanne, CH-1015 Lausanne, Switzerland

ABSTRACT

The consistent infinitesimal finite-element cell method, a boundary finite-element procedure, to model unbounded soil is summarised. This novel procedure based solely on finite elements and standard matrix operations combines the advantages of the boundary-element and finite-element methods. Excellent accuracy for a wide range of problems is demonstrated.

KEYWORDS

Boundary element; Far field; Finite element; Radiation condition; Soil-structure interaction

INTRODUCTION

To analyse dynamic soil-structure interaction by the substructure method, the interaction force-motion relationship in the degrees of freedom on the structure-soil interface of the unbounded soil is required (Fig. 1). In the frequency domain the amplitudes of the displacements $\{u(\omega)\}$ are related to those of

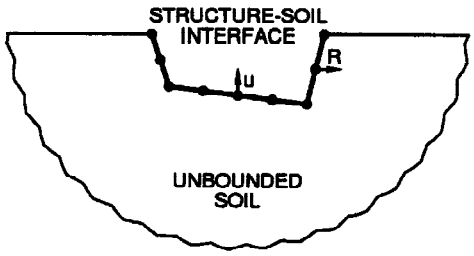

Fig. 1. Interaction force-motion relationship on discretized structure-soil interface of unbounded soil

the interaction forces $\{R(\omega)\}$ by the *dynamic-stiffness matrix* $[S^{\infty}(\omega)]$ as

$$\{R(\omega)\} = [S^{\infty}(\omega)]\{u(\omega)\} \tag{1}$$

In the time domain the convolution integral applies

$$\{R(t)\} = \int_0^t [M^{\infty}(t-\tau)]\{\ddot{u}(\tau)\}\mathrm{d}\tau \tag{2}$$

with the *acceleration unit-impulse response matrix* $[M^{\infty}(t)]$. $[S^{\infty}(\omega)]$ or $[M^{\infty}(t)]$ is calculated with the *consistent infinitesimal finite-element cell method.* As only the structure-soil interface is discretized and the formulation is based solely on finite elements, the method is a *boundary finite-element procedure.*

The consistent infinitesimal finite-element cell method is described in great detail in the book by Wolf and Song (1996), where partial differential equations of the hyperbolic type (e.g. wave propagation in time domain), the parabolic type (e.g. diffusion in time domain) and of the elliptic type (statics and e.g. wave propagation in frequency domain) are addressed. The application to bounded media is also examined. This paper describes only the concept and demonstrates the high versatilities and accuracy in modelling the unbounded soil. For the derivations and a literature survey the reader is referred to Wolf and Song (1996).

CONCEPT

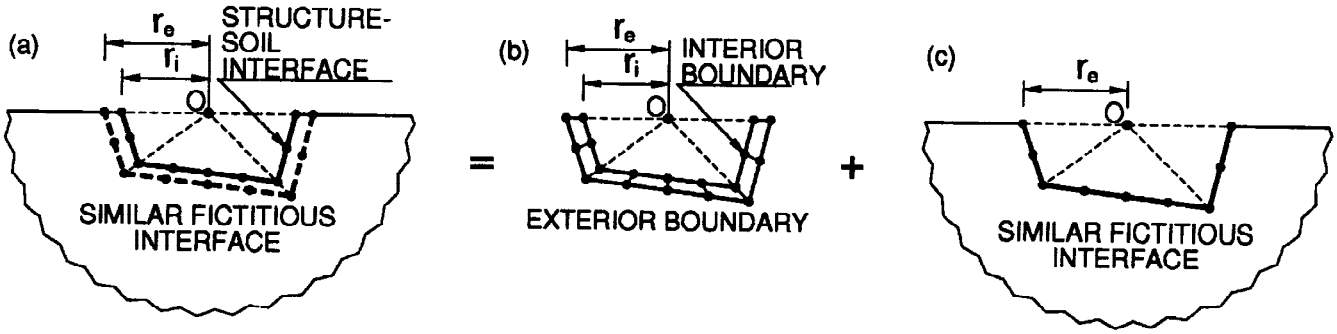

Fig. 2. Concept of consistent infinitesimal finite-element cell method with infinitesimal cell width leading to finite-element discretization of structure-soil interface only

The fundamental idea of the consistent infinitesimal finite-element cell method to model an unbounded soil is illustrated in Fig. 2 taking the irregular structure-soil interface into account. Another *similar* fictitious interface is conceptually introduced by multiplying the coordinates of the structure-soil interface referred to the similarity centre O by a similarity factor (Fig. 2a). The similar interfaces are defined by the characteristic length r, with r_i for the structure-soil interface and r_e for the fictitious interface. The bounded region between these two interfaces is discretized with a cell of finite elements (Fig. 2b) with its interior boundary coinciding with the structure-soil interface and its (similar) exterior boundary with the fictitious interface. The remaining part of the unbounded soil which has not been discretized with finite elements can be interpreted as the same unbounded soil but with the fictitious interface representing another structure-soil interface (Fig. 2c). The latter system is denoted as the unbounded soil characterized by r_e and analogously the actual unbounded soil is characterized by r_i. Obviously, adding the bounded region to the unbounded soil with r_e results in the similar unbounded soil with r_i. This concept can be applied to their dynamic-stiffness matrices. Assembling the dynamic-stiffness matrix of the cell (which is straightforwardly determined from its static-stiffness and mass matrices) and the unknown dynamic-stiffness matrix of the unbounded soil characterized by the length r_e results in the unknown dynamic-stiffness matrix of the unbounded soil with length r_i. This results in one relationship between the dynamic-stiffness matrices at the two interfaces. For an infinitesimal cell width in the radial direction, a term $\partial[S^{\infty}(\omega)]/\partial r$ will occur. In addition, another relationship for the dynamic-stiffness matrices at similar structure-soil interfaces of an unbounded soil is derived using dimensional analysis as

$$r\frac{\partial[S^{\infty}(r,\omega)]}{\partial r} = (s-2)[S^{\infty}(r,\omega)] + \omega\frac{\partial[S^{\infty}(r,\omega)]}{\partial \omega} \tag{3}$$

with the spatial dimension s ($= 2$ or $= 3$). The two relationships leads to an expression for the dynamic-stiffness matrix of the unbounded soil as a function of the property matrices of the cell. Performing the limit of the cell width towards zero analytically yields an equation for the dynamic-stiffness matrix at

the structure-soil interface. Thus, only the discretization of the structure-soil interface remains. The inverse Fourier transformation leads to an equation for the acceleration unit-impulse response matrix.

CONSISTENT INFINITESIMAL FINITE-ELEMENT CELL EQUATION

The structure-soil interface is discretized by doubly-curved surface finite elements. The consistent infinitesimal finite-element cell equation in the frequency domain with the dynamic-stiffness matrix $[S^{\infty}(\omega)]$ as the unknown equals

$$([S^{\infty}(\omega)]+[E^1])[E^0]^{-1}([S^{\infty}(\omega)]+[E^1]^T)-(s-2)[S^{\infty}(\omega)]-\omega\frac{\mathrm{d}[S^{\infty}(\omega)]}{\mathrm{d}\omega}-[E^2]+\omega^2[M^0]=0 \quad (4)$$

The coefficient matrices $[E^0]$, $[E^1]$, $[E^2]$ and $[M^0]$ are calculated and assembled similarly as the static-stiffness and mass matrices of finite elements on the structure-soil interface (Wolf and Song, 1996). For example

$$[E^0]=\int_{-1}^{+1}\int_{-1}^{+1}[B^1]^T[D][B^1]|J|\mathrm{d}\eta\mathrm{d}\zeta \quad (5a)$$

$$[M^0]=\int_{-1}^{+1}\int_{-1}^{+1}\rho[N]^T[N]|J|\mathrm{d}\eta\mathrm{d}\zeta \quad (5b)$$

applies. $[N]$ are the shape functions of the surface finite elements, $|J|$ is associated with the Jacobian matrix, $[B^1]$ follows from the strain-nodal displacement relationship and $[D]$ is the three-dimensional (in general, anisotropic) elasticity matrix of the stress-strain relationship.

This is a system of nonlinear ordinary differential equations of first order. It is solved starting from the boundary condition of $[S^{\infty}(\omega)]$ formulated at a high frequency ω using an asymptotic expansion which permits the radiation condition to be incorporated.

The corresponding equation in the time domain with the acceleration unit-impulse response matrix $[M^{\infty}(t)]$ as the unknown is written as

$$\begin{aligned}\int_0^t[M^{\infty}(t-\tau)][E^0]^{-1}[M^{\infty}(\tau)]d\tau+\left([E^1][E^0]^{-1}-\frac{s+1}{2}[I]\right)\int_0^t\int_0^{\tau}[M^{\infty}(\tau')]d\tau'd\tau\\+\int_0^t\int_0^{\tau}[M^{\infty}(\tau')]d\tau'd\tau\left([E^0]^{-1}[E^1]^T-\frac{s+1}{2}[I]\right)+t\int_0^t[M^{\infty}(\tau)]d\tau\\-\frac{t^3}{6}([E^2]-[E^0]^{-1}[E^1]^T)H(t)-t[M^0]H(t)=0\end{aligned} \quad (6)$$

Applying a time discretization it can be solved step by step. In the first time step a quadratic matrix equation (Riccati equation) is solved, which permits by appropriate choice of the eigenvalues the radiation condition to be incorporated. In all subsequent time steps a linear system of equations with a constant coefficient matrix is solved.

CHARACTERISTIC FEATURES

The consistent infinitesimal finite-element cell method is a *stand-alone finite-element formulation* capable of capturing the radiation condition at infinity without using analytical solutions. Only the coefficient matrices of the surface finite elements are calculated, which are then used in standard matrix operations to obtain the unit-impulse response matrix of the unbounded soil. The method can also calculate problems for which the fundamental solution (which is necessary in the boundary-element method) does not exist in closed form. This is, for example, the case for certain anisotropic materials.

In an actual application the discretization is limited to the structure-medium interface yielding a *reduction of the spatial dimension by one*, as in the boundary-element method. For problems with a boundary extending from the structure-soil interface to infinity (such as a half-space with a free surface) this novel method automatically incorporates this boundary condition in contrast to the boundary-element method. Material inhomogeneities which satisfy similarity can also be processed without any additional effort. When similarity is not satisfied exactly as in Fig. 3a, an approximate representation of

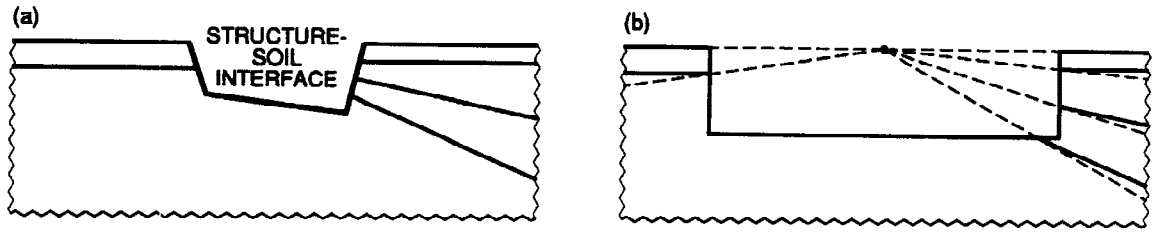

Fig. 3. (a) Original dynamic unbounded soil-structure–interaction problem with layers; (b) Approximate representation enforcing similarity of unbounded soil with structure-soil interface moved outwards

the unbounded soil satisfying similarity as in Fig. 3b can be constructed by moving the structure-soil interface outwards. This procedure should be compared with that of truncating the discretization of the interfaces extending to infinity as used in the boundary-element method.

As no other approximation than that of the finite-element method is introduced, the consistent infinitesimal finite-element cell method *converges to the exact solution in the finite-element sense in the circumferential directions.* Furthermore, as the limit of the infinitesimal cell width is performed analytically, the method is *exact in the radial direction.* The consistent infinitesimal finite-element cell method is thus a *boundary finite-element method* combining the advantages of the boundary-element method and the finite-element method.

The consistent-boundary method (Kausel, Roësset and Waas, 1975) to analyse a horizontally layered medium is a special case of the consistent infinitesimal finite-element cell method where the characteristic lengths of the interior and exterior boundaries are the same.

BENCHMARK EXAMPLES

Examples of increasing complexity with available analytical or other numerical results are calculated with the consistent infinitesimal finite-element cell method. The examples can only be sketched. For details Wolf and Song (1996) should be consulted. The structure-medium interface is discretized with surface finite elements resulting in square matrices $[M^{\infty}(t)]$ or $[S^{\infty}(\omega)]$ of the order of the total number of degrees of freedom. To ease the presentation of the results, a prescribed spatial motion pattern is introduced to calculate the equivalent coefficient. To evaluate $M^{\infty}(t)$ calculated in the time domain using the consistent infinitesimal finite-element cell method, a Fourier transformation is performed which permits $S^{\infty}(\omega)$ to be determined, for which other solutions exist for comparison. $S^{\infty}(\omega)$ is nondimensionalized and then decomposed into the spring coefficient $k(a_0)$ and the damping coefficient $c(a_0)$ with the dimensionless frequency a_0.

Spherical Cavity Embedded in Full-Space

A spherical cavity embedded in a full-space with a uniform radial displacement $u_0(t)$ enforced on the structure-soil interface illustrated in Fig. 4 is analysed with the surface finite-element discretization of the structure-soil interface shown in Fig. 5. For compressible elasticity (Poisson's ratio = 0.25) $M^{\infty}(t)$ is presented in Fig. 6 and for incompressible elasticity (Poisson's ratio = 0.5) the interaction force $R(t)$ resulting from an acceleration step function is plotted in Fig. 7.

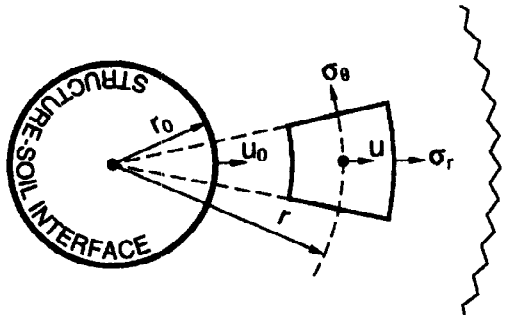

Fig. 4. Spherical cavity embedded in full-space with symmetric waves (section)

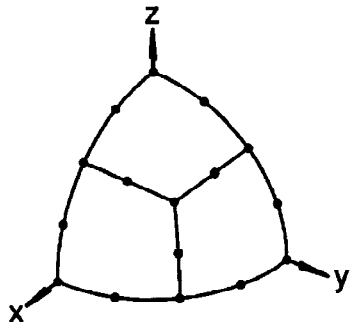

Fig. 5. Finite-element mesh of one octant of structure-soil interface of spherical cavity

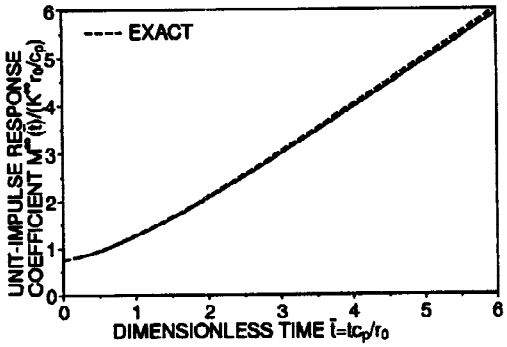

Fig. 6. Acceleration unit-impulse response coefficient for spherical cavity embedded in compressible full-space

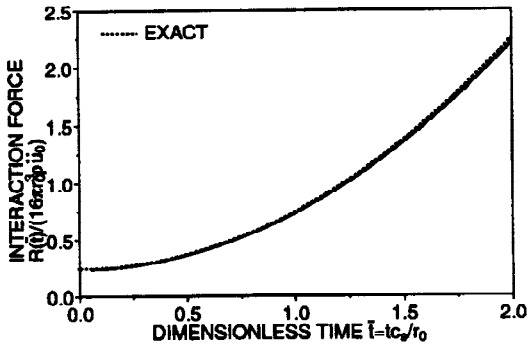

Fig. 7. Interaction force of spherical cavity embedded in incompressible full-space caused by acceleration step function

Circular Cavity Embedded in Full-Plane

A circular cavity embedded in a full-plane with a translational motion $u_0(t)$ enforced on the structure-soil interface shown in Fig. 8 is calculated with 4 3-node line elements per quarter of the structure-soil interface. For compressible elasticity (Poisson's ratio = 1/3) $S^\infty(\omega)$ determined directly in the frequency domain using the consistent infinitesimal finite-element cell method is plotted in Fig. 9. For incompressible elasticity, $M^\infty(t)$ is calculated and then transformed to $S^\infty(\omega)$ shown in Fig. 10.

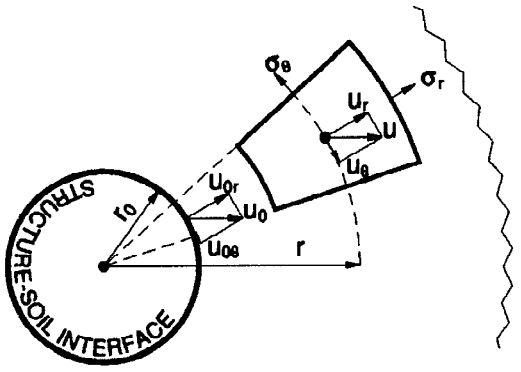

Fig. 8. Circular cavity embedded in full-plane with prescribed translational motion

Semi-Infinite Wedge

The in-plane motion of a semi-infinite wedge with an opening angle = 30°, a free and a fixed boundary and 3 zones of different shear moduli G ($G_1/G_2 = G_3/G_2 = 10$) with a prescribed horizontal displacement shown in Fig. 11 is processed with 6 3-node line elements on the structure-soil interface. $M^\infty(t)$

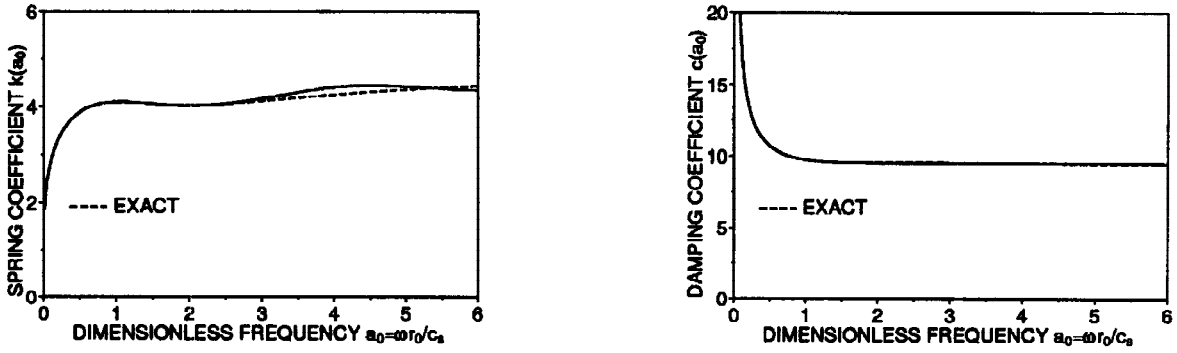

Fig. 9. Dynamic-stiffness coefficient of circular cavity embedded in compressible full-plane calculated directly in frequency domain

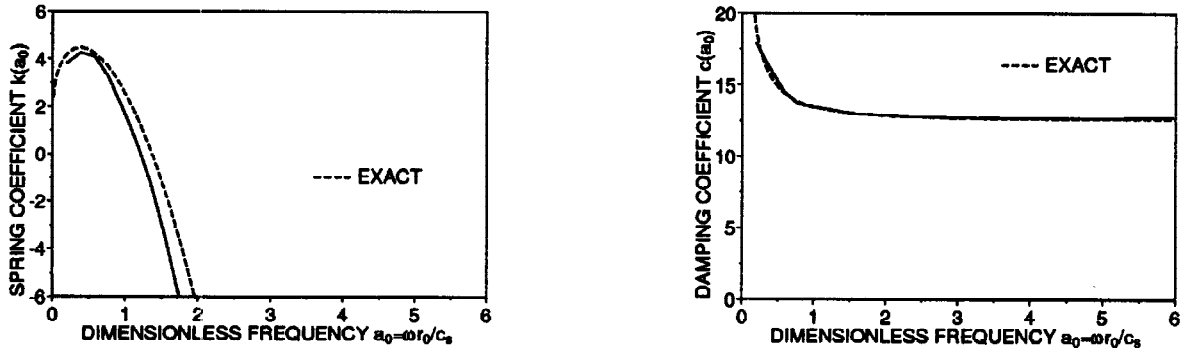

Fig. 10. Dynamic-stiffness coefficient of circular cavity embedded in incompressible full-plane

is plotted in Fig. 12.

Out-of-Plane Motion of Strip Foundation

The out-of-plane (anti-plane) motion of a rectangle ($e = b$) embedded in an inhomogeneous half-plane ($G_2/G_1 = G_2/G_3 = 4$) shown in Fig. 13 is addressed with 24 3-node line elements on the structure-soil interface. $M^{\infty}(t)$ corresponding to twisting of the rigid interface is plotted in Fig. 14.

In-Plane Motion of Strip Foundation

The in-plane motion of a rectangle embedded in a transversely isotropic half-plane shown in Fig. 15 is calculated. The rocking dynamic-stiffness coefficient of a rigid interface $S^{\infty}(\omega)$ determined from $M^{\infty}(t)$ represented in Fig. 16 agrees well with the boundary-element results of Wang and Rajapakse (1991).

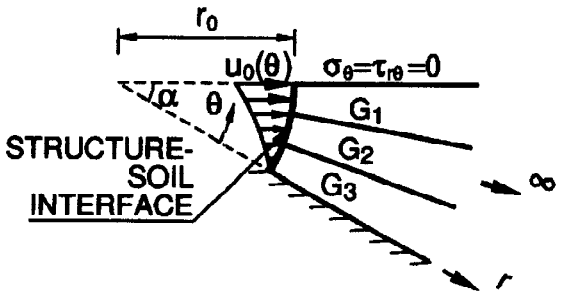

Fig. 11. Inhomogeneous semi-infinite wedge with prescribed horizontal displacement

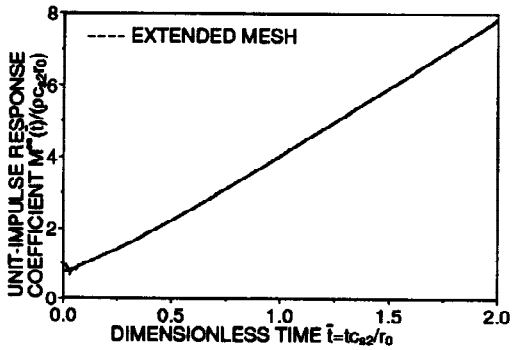

Fig. 12. Acceleration unit-impulse response coefficient of inhomogeneous semi-infinite wedge

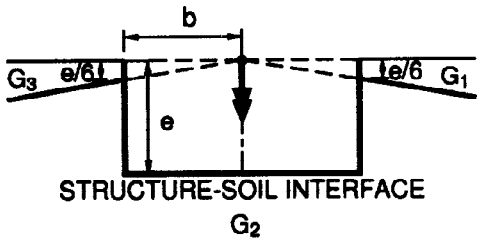

Fig. 13. Out-of-plane motion of strip foundation with rectangular cross section embedded in inhomogeneous half-plane

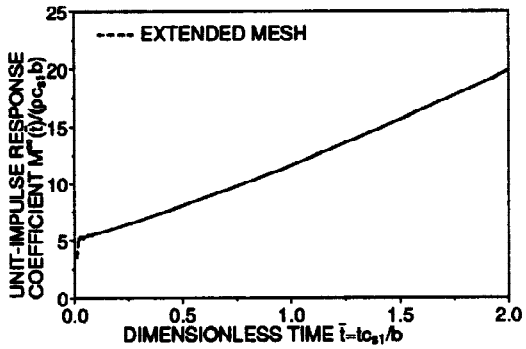

Fig. 14. Acceleration unit-impulse response coefficient of out-of-plane motion of rigid strip foundation embedded in inhomogeneous half-plane

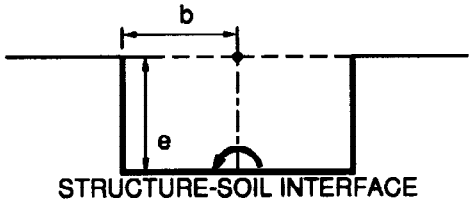

Fig. 15. Strip foundation with rectangular cross section embedded in transversely isotropic half-plane

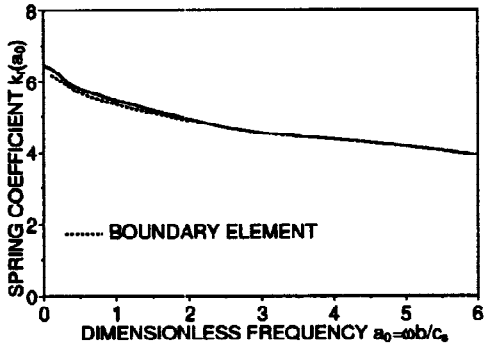

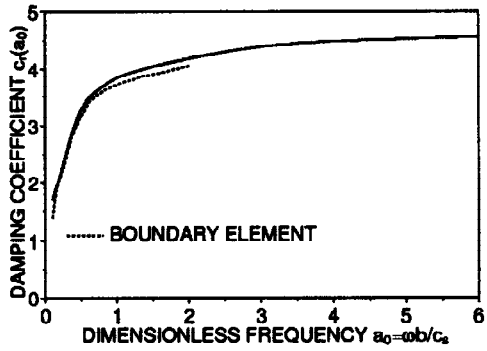

Fig. 16. Rocking dynamic-stiffness coefficient of rigid strip foundation embedded in transversely isotropic half-plane

Prism Embedded in Half-Space

A prism ($e = 2/3b$) embedded in an inhomogeneous half-space ($G_2 = 4G_1$) shown in Fig. 17a is analysed with the finite-element mesh of the structure-medium interface of Fig. 17b. A rigid interface is assumed. The horizontal $S^{\infty}(\omega)$ calculated directly in the frequency domain for the homogeneous case ($G_2 = G_1$) is represented in Fig. 18 with the boundary-element results of Dominguez (1993). The rocking and torsional $M^{\infty}(t)$ for the inhomogeneous case are plotted in Fig. 19.

The results of the consistent infinitesimal finite-element cell method agree very well for a large range of problems with analytical, extended mesh or boundary-element solutions.

REFERENCES

Dominguez, J. (1993) *Boundary Elements in Dynamics*, Computational Mechanics Publications, Southampton.

Kausel, E., Roësset, J. M. and Waas, G. (1975) Dynamic analysis of footings on layered media, *Journal of Engineering Mechanics*, ASCE, *101*, 679–693.

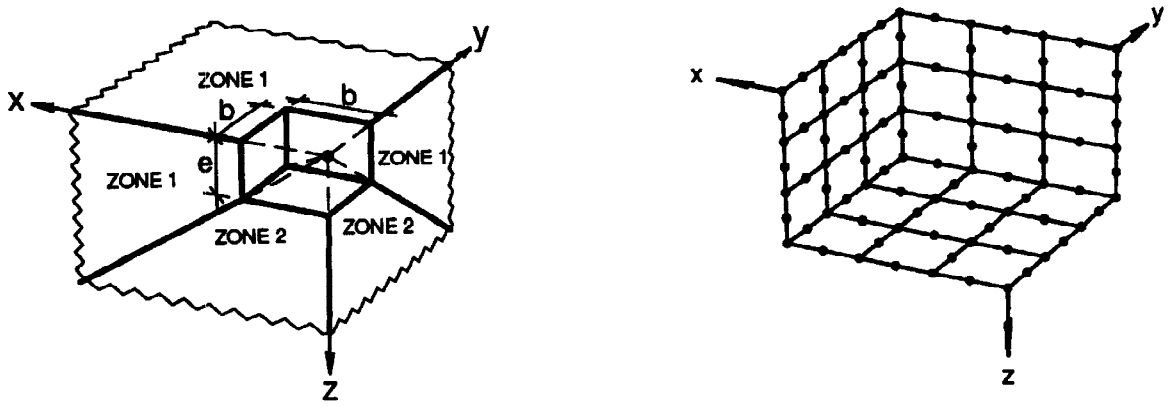

(a) geometry with similarity

(b) finite-element discretization of structure-soil interface

Fig. 17. One quarter of square prism embedded in inhomogeneous half-space

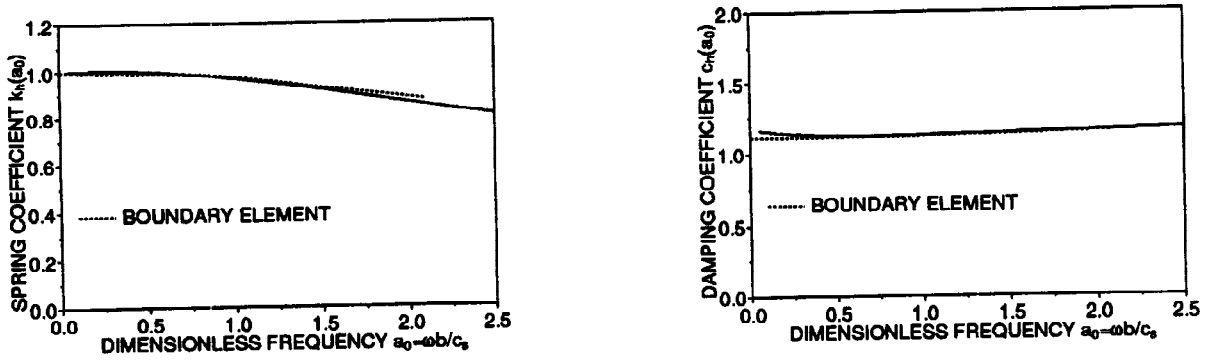

Fig. 18. Horizontal dynamic-stiffness coefficient of rigid prism embedded in homogeneous half-space calculated directly in frequency domain

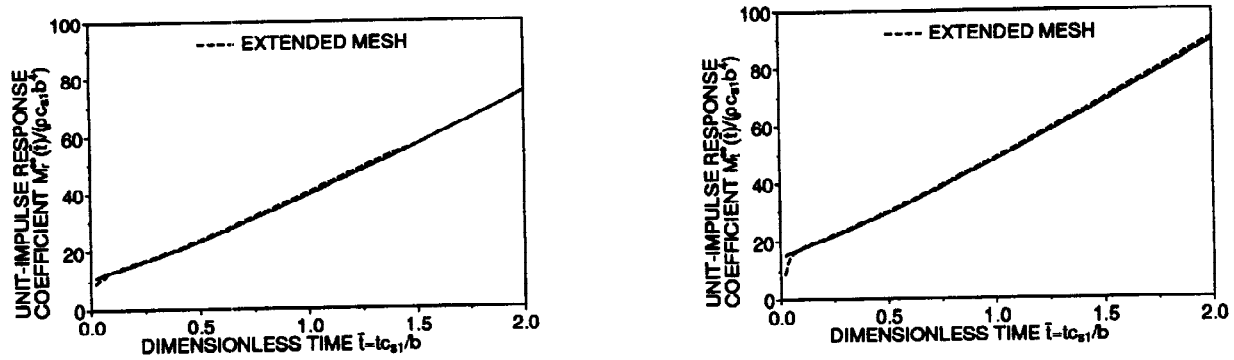

(a) rocking

(b) torsional

Fig. 19. Acceleration unit-impulse response coefficients of rigid prism embedded in inhomogeneous half-space

Wang, Y. and Rajapakse, R. K. N. D. (1991) Dynamics of rigid strip foundations embedded in orthotropic elastic soils, *Earthquake Engineering and Structural Dynamics*, *20*, 927–947.

Wolf, J.P. and Song, Ch. (1996). *Finite-Element Modelling of Unbounded Media*, John Wiley & Sons Ltd.